American Journal of Nano Research and Application
2014; 2(6-1): 1-8
Published online December 19, 2014 (http://www.sciencepublishinggroup.com/j/nano)
doi: 10.11648/j.nano.s.2014020601.11

Tailored nano- and micrometer sized structures of gold-nanoparticles at polymeric surfaces via photochemical and kinetic control of the synthesis and deposition process

Christian Elsner*, Andrea Prager, Ulrich Decker, Sergej Naumov, Bernd Abel

Leibniz Institute of Surface Modification, Chemical Department, Permoser Strasse 15, D-04318 Leipzig, Germany

Email address:
christian.elsner@iom-leipzig.de (C. Elsner)

To cite this article:
Christian Elsner, Andrea Prager, Ulrich Decker, Sergej Naumov, Bernd Abel. Tailored Nano- and Micrometer Sized Structures of Gold-Nanoparticles at Polymeric Surfaces Via Photochemical and Kinetic Control of the Synthesis and Deposition Process. *American Journal of Nano Research and Application.* Special Issue: Advanced Functional Materials. Vol. 2, No. 6-1, 2014, pp. 1-8.
doi: 10.11648/j.nano.s.2014020601.11

Abstract: The goal of the present work is to elucidate complex nano- and micrometer surface modification of soft materials via photochemical and kinetic control of the synthesis and deposition process of gold-nanoparticles. The key to this technology is the synthesis of gold-nanoparticles from different $HAuCl_4$ precursor solutions with photons of a defined short wavelength emitted by Xe_2^* (172 nm) and XeCl* (308 nm) vacuum UV and UV-C excimer lamps. The size and plasmonic properties of the spherical nanoparticles are tailored by the application of different irradiation conditions. Additionally, with 172 nm irradiation porous nanomembranes are generated. Furthermore, the spatial and density controlled immobilization of nanoparticles on to solid supports such as paper and PES membranes is demonstrated leading to defined 2-dimensional structures in the micrometer range. The synthesis of high gold content structures on paper substrates allows for the rapid and simple generation of conductive paths in electronic circuits. The generated micro– and nanosystems are characterized by scanning electron and light microscopy, photoelectron spectroscopy, dynamic light scattering and UV/VIS spectroscopy. In order to shed light into the kinetic mechanism quantum chemical calculations are employed that help to identify preferred reaction paths of the photo-induced reduction of Au(III) to Au(0).

Keywords: Excimer Lamps, Printed Electronics, Conductive Structures, Membranes, UV

1. Introduction

Gold-nanoparticles are among the most extensively studied nanomaterials and have been widely used in several fields.[1] Their size- and shape-dependent optical properties, especially their absorption capacities in the visible region of light based on the surface plasmon resonance (SPR) phenomena of nanoparticles makes them suitable for reporter probes in chemical or biochemical sensors.[2-5] Furthermore, gold-nanoparticles have become attractive in heterogeneous catalysis, imaging agents, hyperthermia medium and LDI mass spectrometry.[6-8] Buttom-up as well as top-down processes for the generation of gold-nanoparticles by radiation techniques, which are clean, one-step, and easy tuneable processes different from conventional chemical ones have been proposed since many years. Radiolysis and photolysis of aqueous $HAuCl_4$-solutions, for instance conducted by the use of a low pressure mercury lamp ($\lambda_{max\ em.}$ = 254 nm) or KrF excimer laser ($\lambda_{max\ em.}$ = 248nm) as well as laser ablation techniques from solid targets are the most suitable approaches.[9-14] Glow discharge techniques are proposed for the generation of highly dispersive and catalytically active gold-nanoparticles in a short timescale and a low technical complexity.[15]

Several techniques exist for the immobilisation of gold-nanoparticles on to solid supports, mainly co-precipitation and impregnation.[16] In the first case the support and the gold-precursor are formed simultaneously, in the latter one the pores of the support are filled with the precursor solution. Thermal treatments, often carried out in air, convert these precursors to elemental, immobilised particles. Consequently, these conventional methods are only suitable for the modification of thermally stable materials, e.g. oxides, and spatial resolved modification as well as integration into a

continuous production process e.g. for the manufacturing of nanoparticle modified web fabrics have serious problems.

In the present study we describe the use of VUV/UVC-excimer lamps for the synthesis of gold-nanoparticles. UV-light provided by the decay of excited dimers is characterised by a single dominant emission band and the absence of any thermal emissions. Depending on the wavelength of the emitted photons strong effects on the treated material can be anticipated, which is limited to a certain penetration depth, typically of a few hundred nanometers into the treated material. Chemical bond dissociation, ionisation and radical formation besides of excitation are the most prominent results of high energy photon interaction with molecules. The short-wavelength photons are especially suited for large area modification of temperature sensitive polymeric materials under normal ambient conditions and have been applied to low-temperature oxidation, photoetching, photodegradation and microstructuring of polymeric surfaces.[17] Moreover, excimer lamps were successfully employed to photodeposition and photoinitiator-free photo-induced free radical polymerisation as well as photoconversion reactions in thin coatings on polymeric substrates.[18-20]

Herein, aqueous solutions of $HAuCl_4$ were exposed to UV-light from Xe_2^*- ($\lambda_{max\ em.}$ = 172nm) and $XeCl^*$- ($\lambda_{max\ em.}$ = 308nm) excimer lamp sources. The obtained gold-nanomaterials were characterized according their size and shape using scanning electron microscopy (SEM) and dynamic light scattering (DLS). Their optical properties were elucidated by UV/VIS spectroscopy. In terms of a technical application the feasibility of the large scale radiation induced synthesis and immobilisation of gold-nanoparticles on web-fabrics was exemplarily demonstrated by the use of paper and membrane flexible substrates. Photoelectron spectroscopy was used to determine the amount of immobilzed particles.

2. Results and Discussion

2.1. Synthesis of Gold-Nanoparticles

Kurihara et al. have studied the process of gold-nanoparticle formation in water and water-in-oil emulsions by pulse radiolysis and laser photolysis and proposed a reduction schema for both systems.[25] The radiolytic generation of elemental gold proceeds via the reduction of Au(III) to Au(II) by solvated electrons (eq. 1'), the disproportionation of Au(II) to Au(III) and Au(I) (eq. 2'), and further reduction of Au(I) to elemental Au (eq. 3'). Recently, a revised multistep reduction mechanism has been proposed by the investigation of gold cluster formation in the presence of iso-propyl radicals which are known as scavengers of oxidising OH-radicals.[26] There, the initial step of reduction of Au(III) is achieved by alcohol radicals (eq. 1) and to a smaller extend by solvated electrons (eq. 1'). The formed Au(II) species disproportionate via the dissociation of a long lived dimer (eq. 2) rather than direct disproportionation (eq. 2'). Moreover, gold cluster formation did not proceed before complete consumption of Au(III). Thus, it is supposed that Au(0) is directly involved in the reduction process of Au(III) after its formation via comproportionation (eq. 4). Consequently, the synthesis of gold-nanoparticles should be inhibited at a constant dose if the amount of Au(III) species is enhanced and exceeds a critical concentration. Based on the investigations of Kurihara et al., the photolytic generation is a multi-photon event and proceeds via the formation of a caged divalent gold complex after excitation, its dissociation and disproportionation followed by a further reduction of the formed monocation to elemental gold.

$$Au^{III} + (CH_3)_2C^{\cdot}OH \rightarrow Au^{III}(CH_3)_2C^{\cdot}OH \rightarrow Au^{II} + (CH_3)_2CO + H^+ \quad (1)$$

$$Au^{III} + e^-_{solv} \rightarrow Au^{II} \quad (1')$$

$$Au^{II} + Au^{II} \rightarrow (Au^{II})_2 \rightarrow Au^{I} + Au^{III} \quad (2)$$

$$Au^{II} + Au^{II} \rightarrow Au^{I} + Au^{III} \quad (2')$$

$$Au^{I} + (CH_3)_2C^{\cdot}OH \rightarrow Au^{I}(CH_3)_2C^{\cdot}OH \rightarrow Au^{0} + (CH_3)_2CO + H^+ \quad (3)$$

$$Au^{I} + e^-_{solv} \rightarrow Au^{0} \quad (3')$$

$$Au^{0} + Au^{III} \rightarrow Au^{I} + Au^{III} \quad (4)$$

$$nAu^{0} \rightarrow Au_n \quad (5)$$

$$Au^{I} + Au_n \rightarrow Au^{I}Au_n \quad (5')$$

$$Au^{I}Au_n + e^-_{solv} \rightarrow Au_{n+1} \quad (5'')$$

$$Au^{I}Au_n + (CH_3)_2C^{\cdot}OH \rightarrow Au_{n+1} + (CH_3)_2CO + H \quad (5''')$$

$$(CH_3)_2CHOH + OH^{\cdot} \rightarrow (CH_3)_2C^{\cdot}OH + H_2O \quad (6)$$

Dependingon the wavelength of the emitted photons from the excimer lamp sources the cleavage of chemical bonds, radical formation and initiation of radiolytic pathways is an option, especially if alcohols are constituents of the reaction mixture. Thus, we have investigated the formation of gold-nanoparticles using irradiation from a Xe_2^* excimer lamp in the presence and absence of *t*-butanol, 2-propanol, ethanol, methanol, and trifluoroethanol under comparable conditions (Figure 1).

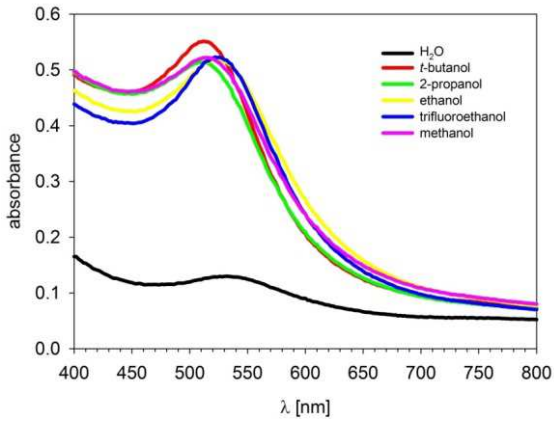

Figure 1. *UV/VIS-absorption spectra of gold-nanoparticles obtained by Xe_2^* excimer irradiation of aqueous $HAuCl_4$ solutions in the presence of different alcohols. Condition I, lamp power: 100 %, irradiation time: 2 min.*

The absorption spectra of the formed nanoparticles present bands with λ_{max} ranging from 512 nm (*t*-butanol) to 532 nm (H_2O). The differences in the absorbance intensity and the position of λ_{max} of the SPR-band can be attributed to differences in the amount and the size of the gold-nanoparticles, respectively.[27] Obviously, the addition of the alcohols promotes the nanoparticle formation. It was already stated that the addition of 2-propanol (but also of ethanol and methanol) has a positive influence on the radiolytic synthesis of gold-nanoparticles according eq. 6. However, we also observed a promotion of nanoparticle formation in the presence of *t*-butanol. The corresponding *t*-butyl radical has no reducing properties. Moreover, the application of photons from $XeCl^*$ excimer lamps which are not able to cleave chemical bonds above 4.2 eV bond dissociation energy (BDE) show a similar behaviour. Thus, the formation of reducing species and the initiation of a radiolytic pathway of gold-nanoparticle formation is presumably not the dominant process. We assume that the used alcohols have a positive influence on the reduction of Au(III) to Au(0) by the promotion of the electron transfer at different stages of the reduction process. Quantum chemical calculation show, that excited solvent molecules may act as electron donors and acceptors and may facilitate the reduction process (Figure 2). Briefly, the $Au(III)Cl_4^-$ anion is formed through the dissociation of the $HAu(III)Cl_4$ molecule (reaction (1)), where the H_2O molecule could act as a proton acceptor. The next step (reaction (2)) may be a direct formation of $Au(III)Cl_3$ through the abstraction of Cl^-. However, this reaction should be energetically unfavorable because of the high Gibbs free energy of the reaction (ΔG = 33.1 kcal mol^{-1}). An alternative way may be the formation of $Au(III)Cl_4$ through a possible electron transfer to the electronically excited solute molecule (CF_3CF_2OH or $CHMe_2OH$) as an electron acceptor, followed by the abstraction of the Cl radical. This reaction could proceed with lower ΔG (ΔG=16 kcal mol^{-1}). The next step (reaction (3)), namely the formation of the $Au(II)Cl_2$ molecule, could proceed either by the disproportionation reaction with the $Au(III)Cl_3$ molecule or by the absorption of the solvated electron (e^-_{solv}) by $Au(III)Cl_3$ followed by the abstraction of the Cl^-. However, the disproportionation reaction is energetically more favorable with ΔG = 15 kcal mol^{-1}. The next step (reaction (4)), namely the formation of the Au(I)Cl molecule, can proceed endergonic both through the disproportionation reaction with the $Au(II)Cl_2$ molecule and through the absorption of the solvated electron (e^-_{solv}) by $Au(II)Cl_2$, followed by the abstraction of the Cl^- . Both of these reactions are exergonic (ΔG = -9 and ΔG = -141 kcal mol^{-1}, respectively) and may possibly proceed spontaneously. The high reactivity of $Au(II)Cl_2$ molecule towards dissociation may be explained by the fact, that $Au(II)Cl_2$ molecule is actually a radical with unpaired number of electrons. It is also in agreement with the experimental finding, that the chemistry of gold is dominated by the oxidation states Au(I) and Au(III). The last step (reaction (5)), the formation of Au(0), could proceed in different ways as shown in

Figure **2**. However, only two ways, namely: 1) the reaction of the solvated electron (e^-_{solv}) with Au(I)Cl followed by the abstraction of the Cl^- and 2) the electron transfer from excited solvent molecules to Au(I)Cl followed by the abstraction of the Cl^-, may be energetically probable. Additionally, the alternative pathway of formation of Au(0) through disproportionation (reaction (6), Figure 2) as proposed in the literature [28] seems to be energetically improbable because of the very high positive Gibbs free energy of the reaction. Thus, it should be mention, that excited solvent molecules may act as electron donors (e-transfer(I)) or acceptors (e-transfer(II)) and may facilitate the reduction process.

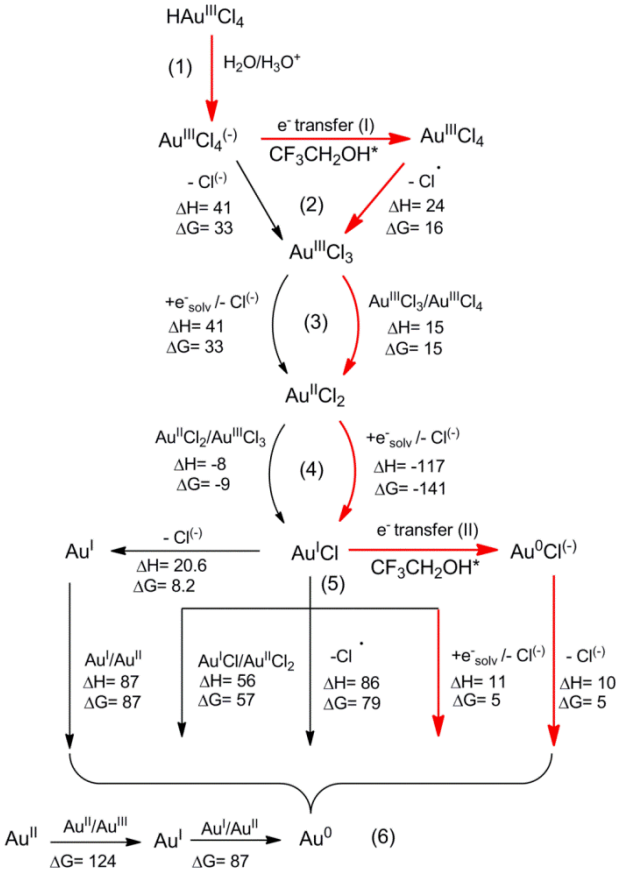

Figure 2.*Transformation scheme for the possible reaction pathways for the Au(0) formation starting from HAu(III)Cl4. The most probable reaction pathway is marked in red. Here, ΔH and ΔG are the reaction enthalpy and Gibbs free energy of the reaction (kcal mol^{-1}) as calculated in water at M06-D/LACV3P+**/PBF level of theory. For further details see the text.*

For further investigations on the photo-induced synthesis of gold-nanoparticles aqueous $HAuCl_4$ solutions in the presence of 2-propanol were used. Depending on the applied dose and wavelength of the emitted VUV-photons different absorbance spectra were obtained for the gold-nanoparticles. A dose influence on λ_{max} of the SPR absorption was observed for the $XeCl^*$-system, whereas for the Xe_2^*-system only a reduction of the absorbance was found (Figure 3). In the case of the $XeCl^*$-system the λ_{max} of the SPR-bands were in the range of 530-580 nm. They were shifted towards longer wavelengths by the reduction of the lamp power (dose). For the Xe_2^*-system λ_{max} of the SPR absorption was around 526 nm independently of the applied dose. The red-shift of λ_{max}in

the case of the $XeCl^*$-excimer lamp irradiation suggests the formation of larger gold-nanoparticles. Indeed, DLS measurements revealed an increase of the particle sizes from 17 nm to 148 nm. The particle sizes after Xe_2^*-excimer lamp irradiation were in the range of 12 nm to 28 nm. Figure 4 shows a plot of the particle sizes versus λ_{max} of the corresponding SPR-absorption in comparison to values obtained from the literature.

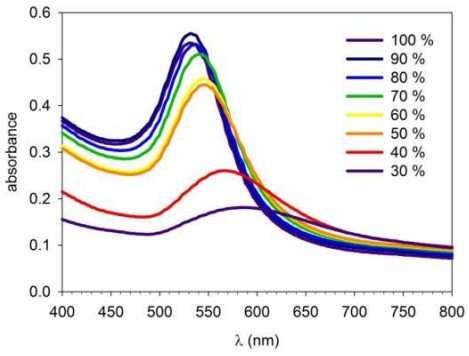

(A)

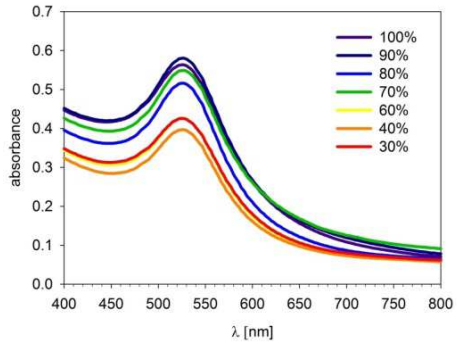

(B)

Figure 3. *UV/VIS-absorption spectra of gold-nanoparticles obtained by $XeCl^*$ (A) and Xe_2^* (B) irradiation of aqueous $HAuCl_4$-solutions at different doses (lamp power). Condition II, lamp power: 100 % - 30 %, irradiation time: 2 min.*

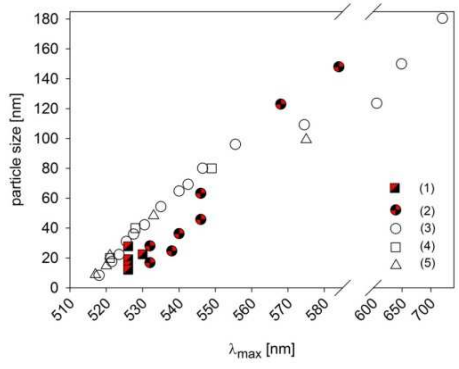

Figure 4. *Comparison of plots of gold-nanoparticle sizes vs. SPR-λ_{max}-values based on data obtained from the literature (3-5, 3: Bastus et al. [29], 4: Jain et al. [30], 5: Link et al. [2]) and synthesized herein by the irradiation of aqueous $HAuCl_4$-solutions using Xe_2^* (1) and $XeCl^*$- (2) excimer lamps. For conditions refer to Figure 3.*

They are in a good agreement; small deviations may be attributed to different crystallinity and shape of the nanoparticles based on the variable preparation methods. The differences of particle sizes obtained during the excimer-lamp irradiation by the Xe_2^*- and $XeCl^*$-system may be explained by the differences in the penetration depths of the photons into the reaction media and the availability of the generated nuclei/seeds and further elemental gold material for coalescence processes in this specific area. The formation of nanoparticles involves competing nucleation processes which proceed above the saturation concentration of elemental gold, and growth processes. The proportion of both determines the final size and shape. Accordingly, if the proportion of seeds to gold atoms suited for growth processes $Au_n/(Au(0)+Au(I))$ becomes smaller, larger particles were obtained. In general, this was observed in the case of $XeCl^*$-excimer lamp irradiation. Comparatively, due to the short wavelength of Xe_2^* derived photons their penetration depth into the reaction liquid is smaller and in general in the range of a few hundred nanometers. Thus, initial processes of gold reduction and particle formation proceed mainly nearby the liquid-gas interface. As a consequence of the absorption of the short wavelength photons in a limited solvent volume the saturation concentration of elemental gold is permanently exceeded and nuclei are formed which preferable take part in coalescence processes if they are impeded in that "Hot zone". Diffusion outside of the "hot zone" reduces the chance for further reduction and coalescence processes dramatically. Consequently, the particle sizes and SPR absorption are in a limited range.

2.2. Synthesis of Porous Gold-Nanomembranes

Increasing the amount of $HAuCl_4$ in the precursor solution, the irradiation with Xe_2^*-excimer lamp derived photons results in an additional formation of a porous nanomembrane due to the preferred particle formation, coalescence and even conversion processes at the interfacial region. The membrane, which appears as a continuous metallic-golden film by the naked eye swimming on top of the reaction liquid, has a thickness of 70 nm (Figure 5). The pores in the range of a few micrometers are not homogeneously distributed over the complete surface area. Especially the border region is characterized by fractal structures and larger pores compared to the more dense structures in the centered regions of the membrane. The grainy, fractal structures suggest a multi-step growth process starting from inter-particle aggregation, domain formation, domain interconnection and the adsorption of further particles, clusters or atoms. To our knowledge, the formation of a metallic, a few tenth nanometer thick membrane by photon induced processes has never been described in the literature. This pronounces the efficiency of excimer lamps for transformation processes which are especially limited to substrate surfaces.

2.3. Immobilisation of Gold-Nanoparticles

Excimer lamps can be used to effectively treat large substrate areas under normal ambient conditions without any high demands on protective or shielding barriers. This is a

clear advantage over other radiation based approaches, e.g. laser and low pressure plasma treatment or even electron beam or gamma irradiation. Since reactive species are only generated in a very thin surface area around 100 nm in depth bulk properties of the substrate will never been altered. As shown herein, the synthesis of gold-nanoparticles by high energy photons from excimer lamp sources proceeds in a short time frame. Thus, the approach seems to be suitable for the synthesis and immobilization of gold-nanoparticles on temperature sensitive web fabrics under roll-to-roll conditions. For this purpose we have used paper and membrane substrates because of their unique open porous structure which facilitates wetting of the precursor solution. Both substrates are considered as interesting and promising materials for the development of disposable diagnostic devices and they became more and more attractive in point-of-care testing.[31, 32] Briefly, a paper and a membrane substrate were immersed with a precursor solution and the wet specimens were passed through the irradiation zone of a series of Xe_2*-excimer lamps using a conveyor system. The absence of thermal emissions prevents the evaporation of volatile liquids such as alcohols, which promote the generation of gold-nanoparticles. A pink colour after irradiation indicated the formation and immobilisation of gold-nanoparticles on the substrate even under non-stationary conditions. A detailed assessment by SEM confirmed the synthesis of gold-nanoparticles on paper and membranes (Figure 6). Although just not studied in detail, the kind of the substrate may play a crucial role in the formation process. Thus, we have observed spherical gold-nanoparticles with a diameter of 20 nm on paper and extremely tiny particles of a few nanometers on the membrane.

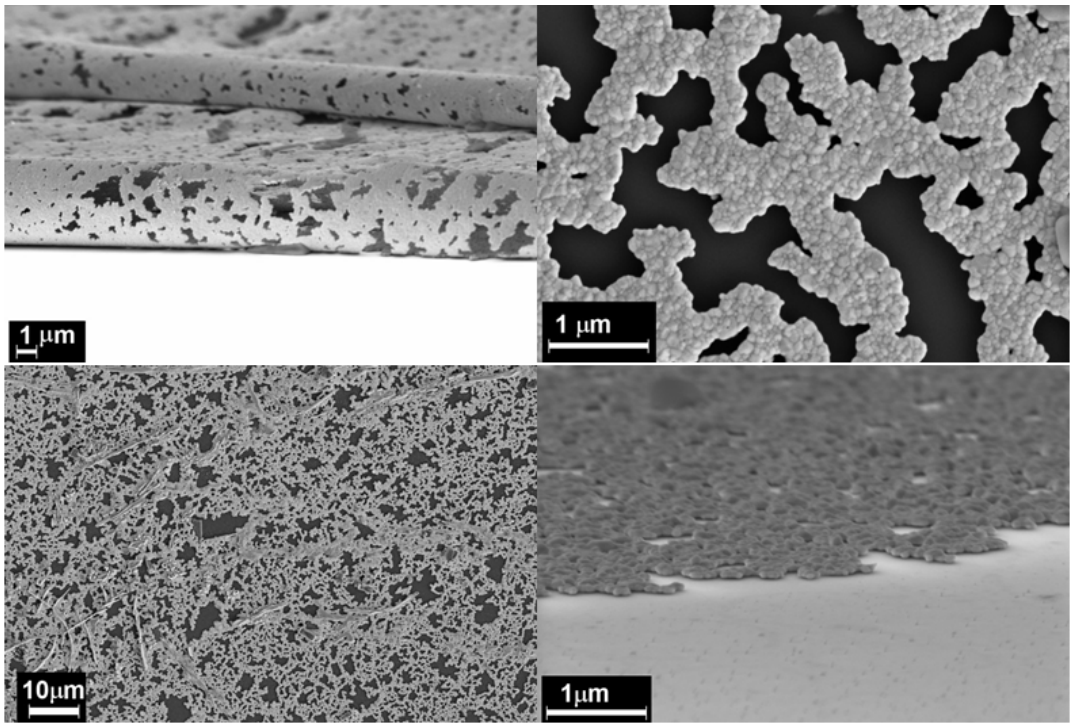

Figure 5. *SEM of porous gold-nanomembrane obtained by the Xe_2^* excimer irradiation of aqueous $HAuCl_4$ solutions. The highly flexible and bendable membrane appears as an interconnected network of sintered nanoparticles. Condition III, lamp power: 100 %, irradiation time: 5 min.*

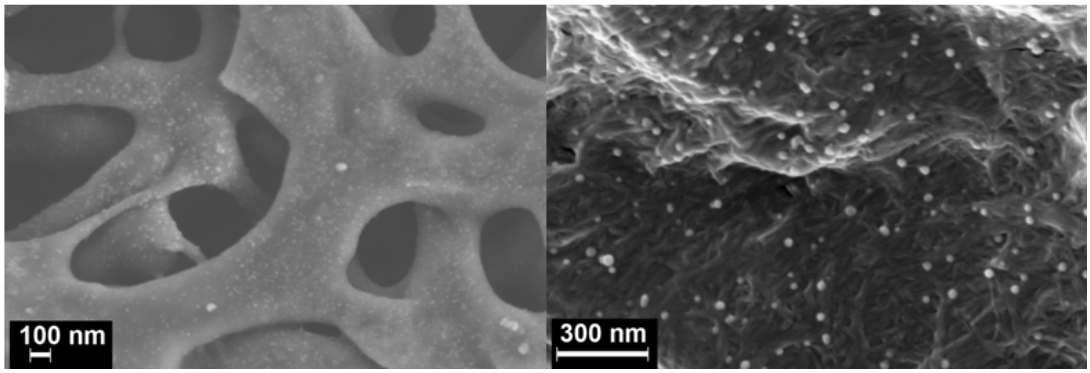

Figure 6. SEM of immobilized gold-nanoparticles on PES-membrane (left) and paper (right) substrates. Condition II.

As a continuation and extension of the experiments we were interested in the spatial resolved immobilisation of nanoparticles on flexible substrates. Photopatterning of structures on the micrometer scale involving nanoparticles

has potential for application to electronic, sensoric and MEMS devices. However, only a few methods for micropatterning of surfaces with nanoparticles exist, mostly based on laser writing.[33] Recently, it has been shown, that the chemistry of the surface can be altered for further structuring and deposition processes by the spatial resolved treatment with short wavelength photons using a photo mask.[34] Herein, we have employed irradiations through a polyimide photo mask for the rapid generation, immobilisation, and arrangement of gold-nanoparticles on paper substrates. The general principle and examples of generated micropatterns on paper substrates are shown in Figure 7.

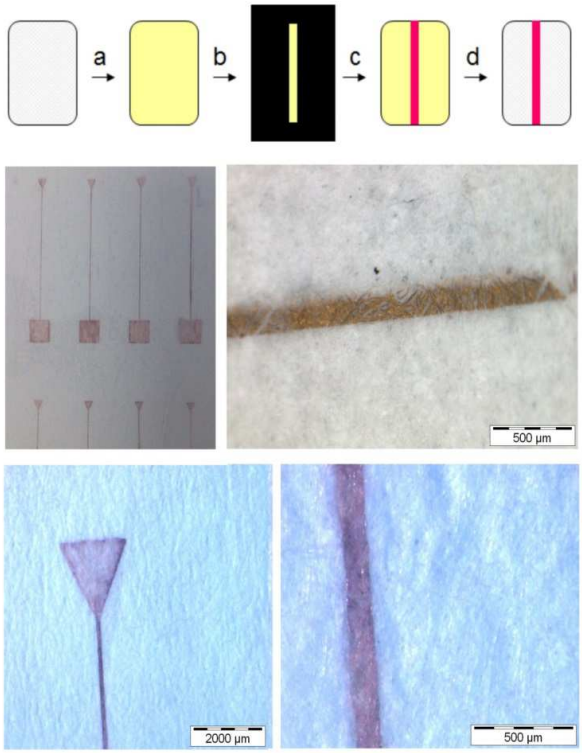

Figure 7. *Schematic of the spatially resolved functionalization of flexible substrates with gold-nanoparticles and examples of 2-dimensional patterns on paper substrates. (a) Immersion of a absorptive flexible substrate with aqueous $HAuCl_4$-solution, (b) application of a photo mask and irradiation, (c) removal of the photo mask, (d) and washing of the substrate with water.*

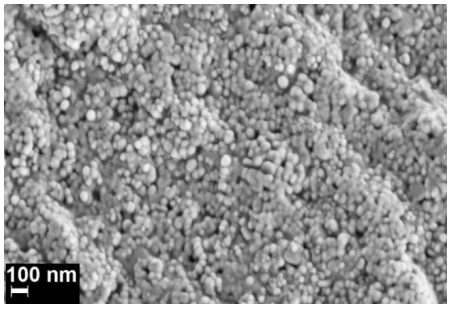

Figure 8. *SEM of a dense gold-nanoparticle film on a paper substrate. The interconnected, presumably sintered aggregates are conductive. The chemical composition [atom-%] of the film was determined by XPS as follows: Au: 32, C: 48, O: 20. Condition IV, lamp power: 100 %, irradiation time: 2 min; two time application.*

Thereby, the density of the formed nanoparticles can be altered from single isolated particles (Figure 7) up to the formation of interconnected grainy nanostructures (Figure 8) appearing as golden-coloured films by the alteration of the concentration of the $HAuCl_4$ in the precursor solution as previously described in the nanomembrane-section.

A detailed investigation was carried out by the determination of the chemical surface composition using photoelectron spectroscopy (XPS). The amount of gold on the surface can be adjusted by the $HAuCl_4$ concentration of the precursor solution as shown in Figure 9.

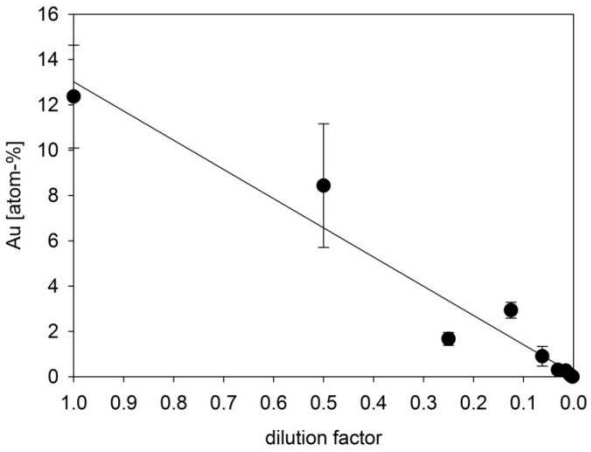

Figure 9. *Atomic concentration of gold on the surface of a paper substrate as a function of the concentration of $HAuCl_4$ in the precursor solution. Condition 5, lamp power: 100 %, irradiation time: 2 min.*

3. Conclusion

In conclusion we have demonstrated the rapid and controlled synthesis of gold-nanoparticles by VUV/UVC-photons of 172 nm and 308 nm wavelength generated by Xe_2*- and XeCl-excimer lamp systems and have applied the approach polymeric substrate surfaces. for the modification of sensitive polymeric substrates. The technique allows for an enhanced control of the synthesi process with respect to time, localization, and density of the formed nanoparticles. The kinetic mechanism for the reduction of the gold precursor has been understood with the help of quantum chemical calculations that enabled us to identify reaction paths of the photo-induced reduction of Au(III) to Au(0). We have developed asuited technology to easily generate complex nano- and micrometer-dimensional structures on soft polymeric surfaces via photochemical and kinetic control of the synthesis and deposition of gold-nanoparticles. Moreover, the immobilization of gold-nanoparticles on suited flexible substrates is not only limited to the lab scale and can in principle be up-scaled to a continuous roll-to-roll process. This may be an important feature for the application of metallic-nanoparticle based systems in the coating or printing industry and allows for alternative approaches of the design of new devices based on the unique properties of nanomaterials.

4. Experimental Section

4.1. Materials

All chemicals and solvents were obtained from commercial sources and used without further purification: 2-propanol (HiPerSolv, HPLC grade), VWR international; methanol, ethanol (Rotisolv, HPLC grad. grade), Carl-Roth GmbH, Karlsruhe, Germany; 2,2,2-trifluoroethanol (synthesis grade), MERCK KGaA, Hohenbrunn, Germany; $HAuCl_4$ (~ 30 wt.% in dilute HCl), Sigma-Aldrich, Germany. For all experiments Millipore-grade water was used. $HAuCl_4$-precursor solutions were prepared by mixing of different amounts (*v/v*) of water, alcohol, and $HAuCl_4$ (~ 30 wt.% in dilute HCl) as follows: Condition I: $HAuCl_4$-stock solution: 7.2 µl $HAuCl_4$ (~ 30 wt.% in dilute HCl) in 5 ml H_2O; working mixture: 275 µl $HAuCl_4$-stock solution, 250 µl H_2O, 25 µl alcohol, condition II: working mixture: 12.5 ml H_2O, 1.25 ml 2-propanol, 9 µl $HAuCl_4$ (~ 30 wt.% in dilute HCl), condition III: working mixture: 982 µl H_2O, 15.6 µl 2-propanol, 2.8 µl $HAuCl_4$ (~ 30 wt.% in dilute HCl), condition IV: working mixture: 98.2 µl H_2O, 1.56 µl 2-propanol, 2.8 µl $HAuCl_4$ (~ 30 wt.% in dilute HCl), condition V: A serial dilution (1:1) was prepared starting from a mixture of 400 µl H_2O, 20 µl 2-propanol, 100 µl $HAuCl_4$ (~ 30 wt.% in dilute HCl) by the addition of the dilution mixture consisting of 4 ml H_2O, 200 µl 2-propanol.

4.2. Excimer Lamp Set Up

Stationary approaches: Open Xe_2^*-excimer irradiation system (λ_{max} = 172 nm, lamp 172/630) and $XeCl^*$-excimer irradiation system (λ_{max} = 308 nm) from Heraeus Noblelight, Kleinostheim, Germany were used. All excimer irradiation experiments were carried out in a nitrogen atmosphere at room temperature and normal pressure. The dose was determined using a Flatlog-system V. 1.2 (Jenoptik Polymer Systems GmbH, Berlin, Germany) with calibrated measuring diodes (GaP: 172 nm, SiC: 308 nm, Figure 10). For the irradiation experiments 96-well microtiter plates (NunclonTM Surface, Nunc, Denmark) with a volume of 0.2 ml/well $HAuCl_4$-precursor solution were used. For non-stationary approaches $HAuCl_4$-precursor solution immersed substrates (paper, membrane) were passed through the irradiation zone of a series of 172 nm excimer lamps using a conveyor system at 2 m min^{-1} applying a dose of 1.7 J/cm^2.

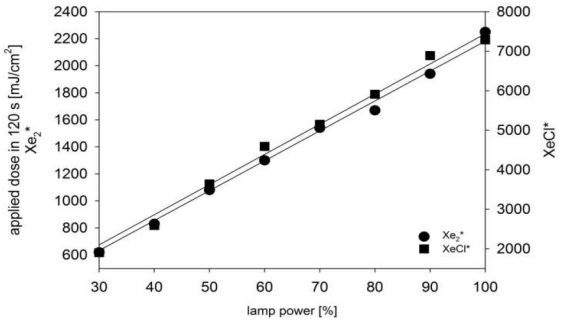

Figure 10. *Applied dose of Xe_2^* and $XeCl^*$-excimer lamps over a period of 120 s at an adjusted lamp power.*

4.3. Instruments

Absorbance spectra in the range of 400 – 800 nm were recorded on a TECAN infinite M 200 microtiter-plate reader using flat bottom micro titer plates and a volume of 0.1 ml/well (Nunclon™ Surface, Nunc, Denmark). DLS measurements were performed on a MALVERN Nanoseries Nano ZS zetasizer. Scanning electron micrographs were generated on an ULTRA 55 Carl Zeiss SMT.

4.4. Computational Methods

Density Functional Theory (DFT) calculations were carried out using the M06-D3 density functional. MO6 functional is parameterized for organometallic and noncovalent interactions (Zhao and Truhlar, 2008).[21] M06-D3 functional includes physically and chemically very important London dispersion interactions (Grimme et al., 2010).[22] The molecular geometries and energies of the all calculated molecules were calculated at the M06-D3/LACV3P+** level of theory as implemented in Jaguar 8.1 program (Jaguar 8.1, 2013). The LACV3P+** basis set uses the standard 6-311+G** basis set for light elements and the LAC pseudopotential (Wadt and Hay, 1985) for the heavier elements, such as Au in this case.[23] Frequency calculations were done at the same level of theory to characterize the stationary points on the potential surface and to obtain total enthalpy (H) and Gibbs free energy (G) at a standard temperature of 298.15 K using un-scaled vibrations. The reaction enthalpies (ΔH) and Gibbs free energies of reaction (ΔG) were calculated as the difference of the total enthalpy H and the Gibbs free energies G between the reactants and products, respectively. To take solvent effect on the structure and reaction parameters of studied molecules into account the calculation were done using Jaguar's dielectric continuum Poisson-Boltzmann solver, which fits the field produced by the solvent dielectric continuum to another set of point charges (Tannor et al.).[24]

Acknowledgements

The work was supported by the Federal Government of Germany and the Freistaat Sachsen.

References

[1] Daniel, M. C.; Astruc, D., *Chem Rev* 2004, *104* (1), 293-346. DOI 10.1021/cr030698+.

[2] Link, S.; El-Sayed, M. A., *Journal of Physical Chemistry B* 1999, *103* (21), 4212-4217. DOI 10.1021/jp984796o.

[3] Link, S.; El-Sayed, M. A., *Int. Rev. Phys. Chem.* 2000, *19* (3), 409-453. DOI 10.1080/01442350050034180.

[4] Watanabe, S.; Yamamoto, S.; Yoshida, K.; Shinkawa, K.; Kumagawa, D.; Seguchi, H., *Supramolecular Chemistry* 2011, *23* (3-4), 297-303. DOI Pii 936375251Doi 10.1080/10610278.2010.527977.

[5] Stewart, M. E.; Anderton, C. R.; Thompson, L. B.; Maria, J.; Gray, S. K.; Rogers, J. A.; Nuzzo, R. G., *Chemical Reviews* 2008, *108* (2), 494-521. DOI 10.1021/cr068126n.

[6] Boronat, M.; Corma, A., *Journal of Catalysis* 2011, *284* (2), 138-147. DOI DOI 10.1016/j.jcat.2011.09.010.

[7] Della Pina, C.; Falletta, E.; Rossi, M., *Chem Soc Rev* 2012, *41* (1), 350-69. DOI 10.1039/c1cs15089h.

[8] Haruta, M.; Date, M., *Applied Catalysis a-General* 2001, *222* (1-2), 427-437.

[9] Belloni, J.; Mostafavi, M.; Remita, H.; Marignier, J. L.; Delcourt, M. O., *New Journal of Chemistry* 1998, *22* (11), 1239-1255. DOI 10.1039/a801445k.

[10] Henglein, A., *Langmuir* 1999, *15* (20), 6738-6744. DOI 10.1021/la9901579.

[11] Sau, T. K.; Pal, A.; Jana, N. R.; Wang, Z. L.; Pal, T., *Journal of Nanoparticle Research* 2001, *3* (4), 257-261. DOI 10.1023/a:1017567225071.

[12] Esumi, K.; Matsuhisa, K.; Torigoe, K., *Langmuir* 1995, *11* (9), 3285-3287. DOI 10.1021/la00009a002.

[13] Watanabe, M.; Takamura, H.; Sugai, H., *Nanoscale Res. Lett.* 2009, *4* (6), 565-573. DOI 10.1007/s11671-009-9281-2.

[14] Biswal, J.; Ramnani, S. P.; Shirolikar, S.; Sabharwal, S., *Radiat. Phys. Chem.* 2011, *80* (1), 44-49. DOI 10.1016/j.radphyschem.2010.08.016.

[15] Liang, X.; Wang, Z. J.; Liu, C. J., *Nanoscale Res. Lett.* 2010, *5* (1), 124-129. DOI 10.1007/s11671-009-9453-0.

[16] Bond, G. C.; Louis, C.; Thompson, D. T., Preparation of Supported Gold Catalysts. In *Catalysis by Gold*, Hutchings, G. J., Ed. Imperial College Press: 2006; Vol. 6, pp 72-120.

[17] Kogelschatz, U., *Appl. Surf. Sci.* 1992, *54* (C), 410-423.

[18] Scherzer, T.; Knolle, W.; Naumov, S.; Mehnert, R., *Nucl. Instr. Meth. Phys. Res. B.* 2003, *208* (1-4), 271-276.

[19] Elsner, C.; Lenk, M.; Prager, L.; Mehnert, R., *Appl. Surf. Sci.* 2006, *252* (10), 3616-3624.

[20] Prager, L.; Dierdorf, A.; Liebe, H.; Naumov, S.; Stojanovic, S.; Heller, R.; Wennrich, L.; Buchmeiser, M. R., *Chem. Eur. J.* 2007, *13* (30), 8522-8529.

[21] Zhao, Y.; Truhlar, D. G., *Theoretical Chemistry Accounts* 2008, *120* (1-3), 215-241. DOI 10.1007/s00214-007-0310-x.

[22] Grimme, S.; Antony, J.; Ehrlich, S.; Krieg, H., *Journal of Chemical Physics* 2010, *132* (15). DOI 10.1063/1.3382344.

[23] Wadt, W. R.; Hay, P. J., *Journal of Chemical Physics* 1985, *82* (1), 284-298. DOI 10.1063/1.448800.

[24] Tannor, D. J.; Marten, B.; Murphy, R.; Friesner, R. A.; Sitkoff, D.; Nicholls, A.; Ringnalda, M.; Goddard, W. A.; Honig, B., *Journal of the American Chemical Society* 1994, *116* (26), 11875-11882. DOI 10.1021/ja00105a030.

[25] Kurihara, K.; Kizling, J.; Stenius, P.; Fendler, J. H., *Journal of the American Chemical Society* 1983, *105* (9), 2574-2579. DOI 10.1021/ja00347a011.

[26] Dey, G. R.; El Omar, A. K.; Jacob, J. A.; Mostafavi, M.; Belloni, J., *J. Phys. Chem. A* 2011, *115* (4), 383-391. DOI 10.1021/jp1096597.

[27] Huang, W. C.; Chen, Y. C., *Journal of Nanoparticle Research* 2008, *10* (4), 697-702. DOI DOI 10.1007/s11051-007-9293-8.

[28] Shang, Y. Z.; Min, C. Z.; Hu, J.; Wang, T. M.; Liu, H. L.; Hu, Y., *Solid State Sci.* 2013, *15*, 17-23. DOI 10.1016/j.solidstatesciences.2012.09.002.

[29] Bastus, N. G.; Comenge, J.; Puntes, V., *Langmuir* 2011, *27* (17), 11098-11105. DOI 10.1021/la201938u.

[30] Jain, P. K.; Lee, K. S.; El-Sayed, I. H.; El-Sayed, M. A., *Journal of Physical Chemistry B* 2006, *110* (14), 7238-7248. DOI 10.1021/jp057170o.

[31] Rozand, C., *Eur. J. Clin. Microbiol. Infect. Dis.* 2014, *33* (2), 147-156. DOI 10.1007/s10096-013-1945-2.

[32] Veigas, B.; Jacob, J. M.; Costa, M. N.; Santos, D. S.; Viveiros, M.; Inacio, J.; Martins, R.; Barquinha, P.; Fortunato, E.; Baptista, P. V., *Lab on a Chip* 2012, *12* (22), 4802-4808. DOI 10.1039/c2lc40739f.

[33] Spano, F.; Castellano, A.; Massaro, A.; Fragouli, D.; Cingolani, R.; Athanassiou, A., *Journal of Nanoscience and Nanotechnology* 2012, *12* (6), 4820-4824. DOI 10.1166/jnn.2012.4931.

[34] Elsner, C.; Naumov, S.; Zajadacz, J.; Buchmeiser, M. R., *Thin Solid Films* 2009, *517* (24), 6772-6776. DOI 10.1016/j.tsf.2009.05.041.